1-1-1987

Metamorphic Veins in the Paleozoic Rocks of Central and Northern Vermont

Anderson, James R.

METAMORPHIC VEINS IN THE PALEOZOIC ROCKS OF CENTRAL AND NORTHERN VERMONT

James R. Anderson
Department of Chemistry, Arizona State University
Tempe, Arizona 85287

INTRODUCTION

The trip will examine the petrology and structural setting of metamorphic veins formed during the Taconic and Acadian Orogenies in the Paleozoic rocks of central and northern Vermont. In the Cambro-Ordovician rocks on the east limb of the Green Mountain anticlinorium in central Vermont, four generations of veins with primary metamorphic assemblages are found. In the Siluro-Devonian rocks of the Brownington syncline and the Strafford-Willoughby arch, two prominent generations of metamorphic veins are present. For each vein generation, much of the mineral growth apparently occurred as metamorphic grade was decreasing from the peak conditions of the metamorphic event with which it was associated. Due to time constraints and the lack of access to many of the best studied outcrops in the younger rocks (roadcuts on I-89 and I-91), the trip will primarily focus on the metamorphic veins in the Cambro-Ordovician rocks.

The two major Paleozoic orogenic episodes each consisted of a sequence of tectonic events that involved both deformation and metamorphic mineral growth. Various approaches have been used to decipher the tectonic history of the region. Many studies have emphasized structural aspects, others have been concerned with petrologic aspects, and some have tried to combine both. The approach used here combines petrologic and structural evidence and attempts to make a direct correlation of deformational and mineral growth features by using several generations of prominently developed metamorphic veins. Use of metamorphic veins in northern Vermont as structural and petrologic markers was initially outlined by Anderson and Albee (1975).

The study of the polymetamorphic history of central Vermont by White and Jahns (1950) was the first detailed work of its kind done in the study area. They and most others that followed relied primarily on the sequence of superimposed deformational elements, in particular the sequence of folds and s-surfaces. Cady (1969) summarized most of the other previous work in the area. Modifications to the earlier views of the deformational history of northern Vermont have been discussed by Albee (1972) and Anderson (1977a).

The presence of more than one distinctly separate generation of metamorphic mineral growth has long been recognized in the study area. Albee (1968) and Lanphere and Albee (1974) established the presence of at least two generations, one or more generations of Ordovician age and one or more of Devonian age. Laird (1977) and Laird and Albee (1981a, 1981b) have shown the presence of multiple generations of amphiboles in the Paleozoic mafic schists of Vermont and have used amphibole compositions to show differences in baric types of the different generations.

The interpretation of systematic compositional variation in chemically zoned mineral grains is a central concern of this study. Zoning could have been produced by growth during changing physical and/or chemical conditions or by solid-state diffusion after growth or by some combination of the two. Systematic variation that is complex was most likely produced by growth over a period of changing conditions (Anderson, 1977b).

All compositional data discussed were acquired on automated electron microprobes using wavelength-dispersive spectrometers. Analytical and data treatment methods of this study have been discussed by Anderson (1983).

Structural setting of the veins

The structural setting of the metamorphic veins area can be described by considering orientation, form, size, and position within the sequence of superimposed deformational elements. The younger vein generations, the least distorted by superimposed deformation, exhibit a variety of forms including lens-shaped veins parallel to an axial-plane s-surface, en echelon gash veins, veins which fill irregular pull-apart structures of several sorts, and sheet-like fracture-filling veins. One vein generation may have several types of forms that vary in predominance from one part of the area to another or vary locally with rock type. Most of the major vein generations are

geometrically related to s-surfaces, but the minor vein generations and one major generation are not. This latter major generation of relatively undeformed veins is related to late mineral growth in the host rocks. The minor vein generations have no apparent relationship to mineral growth in the host rock and are almost invariably of very simple mineralogy, such as quartz only or quartz and calcite.

Even for a single major vein generation considerable variability is observed in the proportional relationships between the smallest dimension (the "width"), the intermediate dimension (not appropriate for sheet-like veins), and the largest dimension. For veins parallel to an s-surface, the smaller dimension is generally perpendicular to the s-surface. The largest dimension in many cases is roughly parallel to hinges of folds related to the s-surface, but shear folding appears to be the dominant fold mechanism and there is not always a clearcut relationship between one of the larger vein dimensions and the fold hinges. Vein widths may be as small as 1-2 mm or as large as 1 m or more. The other two dimensions have similar large variability and for the larger veins both may extend beyond the limits of the exposed rock. The older vein generations are not uncommonly highly deformed and consequently their original size, form, and orientation are difficult to determine.

Some veins of each recognized generation can be shown to be discontinuous in extent on the scale of a few tens of meters or less. Discontinuous veins are petrologically and texturally the same as veins of the same generation that cannot be shown to be discontinuous because the outcrops are small or the veins very large. Veins of the major generations appear to be localized, isolated features that grew in discontinuous tension fractures rather than elements in a large-scale hydrothermal network.

The mechanics of the formation of metamorphic veins and tension fractures in general under high confining pressures have been discussed by a number of authors (for example, Secor, 1969; Beach 1975, 1977; Etheridge, 1983). The tension fractures in which the veins grow cannot form when the differential stress exceeds some upper limit. Etheridge (1983) has estimated the upper limit to be not more than 400 bars and probably closer to 100 bars for typical regional metamorphic rocks. Therefore high relative fluid pressure, close to the confining pressure, was required for vein initiation and growth.

The designation of the structural elements used here is not the standard system of S_1, S_2, F_1, and so on, in part because of the complications presented by the major unconformity in the middle of the study area between Ordovician and Silurian units. S_1 on one side of the unconformity is not equivalent to S_1 on the other side. Also, in the standard system different types of structural elements with the same subscript have no implied genetic relationship so that in dealing with elements interpreted to be cogenetic, the discussion can get quite complex. For the description that follows, letters are used as subscripts and those elements with the same subscript are, based on geometric relationships, interpreted to be cogenetic or at least to all occupy the same position in relative time as determined by their position in the structural sequence of superimposed elements. The oldest group of elements are subscripted "a", the next oldest "b", and so on. This usage will differ from the standard system if any group of cogenetic elements does not contain all types of structural elements.

Examples from Stops in Cambrian and Ordovician rocks

Stops 1 through 4 (Fig. 1 and Itinerary) are in pelitic schists of the Hazens Notch and Underhill formations, Cambrian in age, on the east limb of the Green Mountain anticlinorium. All lie on the high-grade side of the garnet isograd mapped by Christman and Secor (1961). Stops 5 and 9 are outcrops of amphibolite of the Stowe formation, Ordovician in age, from the N-S trending area of garnet-grade through sillimanite-muscovite-grade rocks that coincides with the Worcester Mountains (Cady, 1956; Albee, 1957, 1968; Anderson, unpub. data).

Stops 1-4: Structural Sequence

The structural sequence at Stop 1 is a good starting point for discussion. The oldest secondary s-surface is a highly deformed schistosity, S_a, that at some locations is parallel to original compositional layering (a good example is at Stop 7). At Stop 1 the primary layering has been obscured by metamorphism. S_a is not related to any small folds observed in the area. Parallel to S_a are metamorphic veins that are generally not more than about 10 cm wide and of indeterminate larger dimensions because of strong deformation. These veins, V_a, are isoclinally folded by large

and small tight folds to which the predominant schistosity, S_b, in the pelitic schists is axial-planar. The isoclinal folds, F_b, have hinges that generally trend E-W within S_b, but S_b and F_b are deformed by younger folding so that the orientations of S_b and hinges of F_b are highly variable. Parallel to S_b and therefore axial planar to F_b are metamorphic veins, V_b. Superimposed on S_b, F_b, and V_b are asymmetric folds with N-S axial trends. These are F_c folds and have associated with them an axial-plane slip cleavage, S_c, for which the degree of development varies considerably in the outcrop. In this part of the study area, S_c slip cleavage is generally better developed on the short limbs of the asymmetric F_c folds than on the long limbs, but the rock type is also a factor. Parallel to S_c slip cleavage and commonly within the axial regions of small F_c folds are lens-shaped veins, V_c. The small F_c folds appear to be related to the larger N-S fold structures of the Green Mountain anticlinorium in this area (I avoid the unfortunate term "Green Mountain folds").

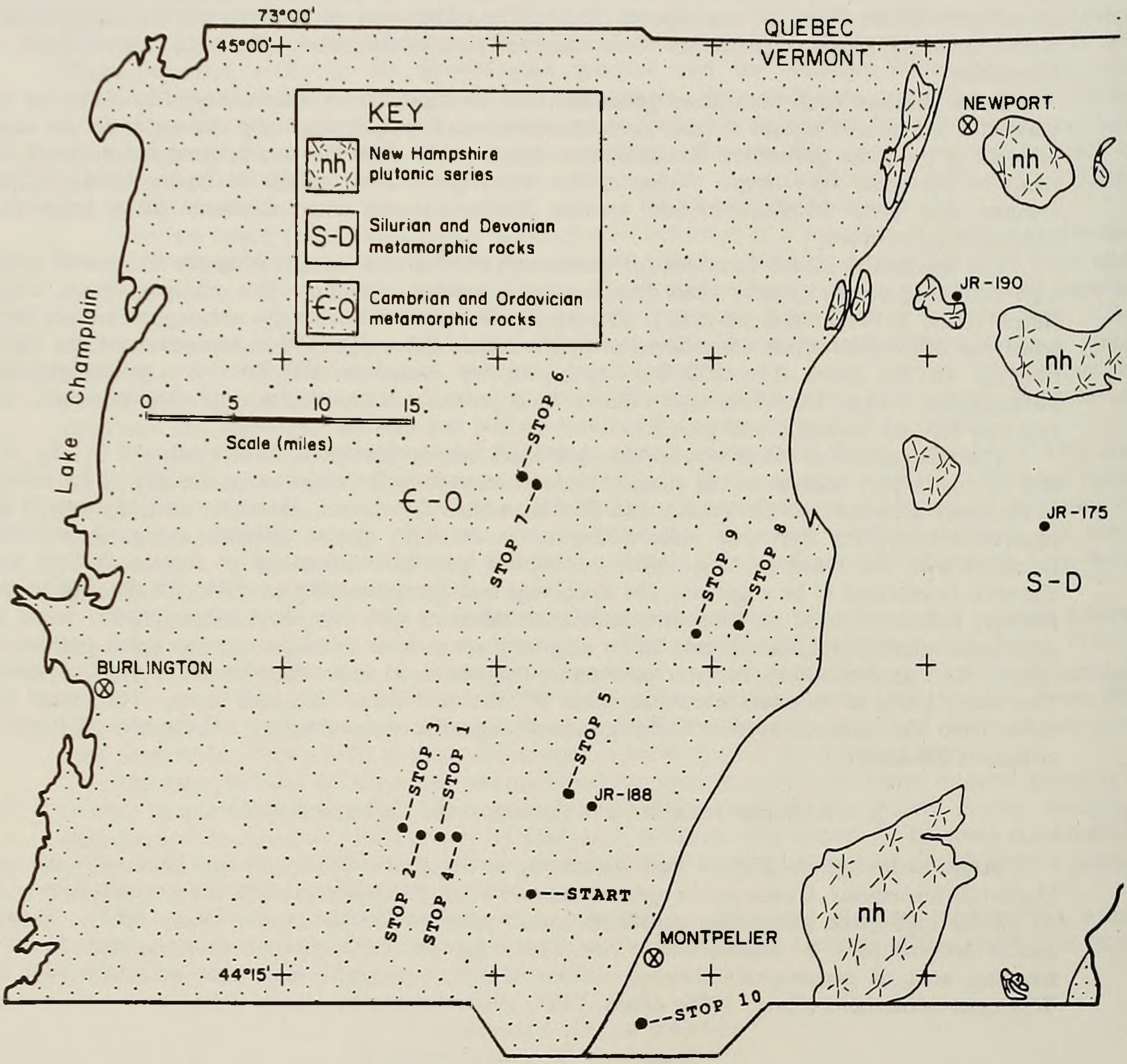

Figure 1. Sketch map of the study area with stops indicated.

S_c cleavage and associated V_c veins are gently folded by open, asymmetric folds (F_d) with N-S to NNE-SSW axial trends. F_d folds are not visibly developed in all parts of the outcrop and vary in development at nearby outcrops. At outcrops where the folds are better developed than at Stop 1, a slip cleavage, S_d, is parallel to F_d axial planes. Where present, S_d is superimposed on the nearly

ubiquitous S_c slip cleavage. Unlike the other s-surfaces, S_d does not have any associated parallel metamorphic veins. The absence of a vein set in this position of the structural sequence is consistent throughout the studied area of Cambrian and Ordovician rocks in northern Vermont.

A fourth major vein generation, designated V_e, is found at Stop 3 and other nearby outcrops. V_e veins crosscut all of the structural elements described above. V_e veins are not associated with any s-surface or fold set but have mineral assemblages within them that are subsets of assemblages of late retrograde minerals in the host rocks. The structural sequence for Stops 1-4 (also applicable to 5-9) is summarized in part A of Table 1.

The superposition relationships among major vein generations is as clear as those among other structural elements. The possibility that a vein parallel to an older s-surface, say V_b parallel to S_b, could have formed at the same time as or later than a superimposed s-surface, say S_c, is ruled out by the way in which the superimposed s-surfaces and folds affect the veins. All the fold generations appear to have formed by mechanisms that mainly involved shear folding, so the presence of tension fractures parallel to folded, pre-existing s-surfaces at high angles to the axial surfaces is much less likely than would be the case if flexure folding were important.

Vein and host rock mineral growth at Stop 1 (location JR-5)

Hazens Notch schist at Stop 1 has the assemblage quartz, plagioclase, muscovite, chlorite, epidote, apatite, ilmenite, pyrrhotite, and zircon with or without garnet, calcite, chalcopyrite, tourmaline, and/or pyrite. Garnet is replaced to varying extent by randomly oriented grains of chlorite with minor muscovite, most extensively in samples with best-developed S_c slip cleavage. Chlorite and muscovite grains with preferred orientation parallel to S_c are in several samples. Some of the grains have been rotated into this position by microfolding of the S_b schistosity and some appear to have grown in this position, crosscutting the microfolded schistosity.

Veins of the three different generations have assemblages that are subsets of the assemblages of adjacent host rocks. Important minerals in all three are quartz, plagioclase, chlorite, and minor muscovite. One or more of the following may also be present in generally minor amounts: ilmenite, apatite, pyrrhotite, calcite, and chalcopyrite. In V_b and V_c veins, secondary pyrite after pyrrhotite and secondary muscovite and paragonite after plagioclase occur in minor but varying amounts. The less deformed veins of the V_b and V_c generations generally have very coarse mineral grains, up to 10 cm or more in greatest dimension, and lack the strong directional fabric that typifies the schist. Many of the coarse grains of vein plagioclase are euhedral to subhedral, in contrast to anhedral porphyroblasts in the schist. Vein chlorite grains are larger than grains in the schist and lack preferred orientation; many are fan-like or accordian-like in form. By comparison to the younger veins, the highly deformed V_a veins appear to have undergone substantial recrystallization and grain-size reduction. Grain sizes and forms in V_a veins are more comparable to those in the schist and also the platy minerals not uncommonly have preferred orientation parallel to S_b.

Samples from a V_b vein - JR-5-A & JR-5-B

Sample JR-5-A includes the edge of the V_b vein and adjacent schist, whereas JR-5-B is from the center of the vein. The vein assemblage is quartz, plagioclase, chlorite, muscovite, calcite, ilmenite, apatite, pyrrhotite partly replaced by pyrite, and chalcopyrite. The contact between the vein and schist is relatively sharp and is grossly parallel to S_b schistosity. The adjacent schist has well-developed S_b schistosity but lacks S_c slip cleavage. The schist has an assemblage that includes the vein minerals plus zircon and tourmaline. Modal abundances of the major minerals are very different in the vein and adjacent schist.

Typical plagioclase porphyroblasts in the host schist in JR-5-A are anhedral and elongate parallel to S_b in contrast to the euhedral and subhedral porphyroblasts in the adjacent V_b vein. Schist porphyroblasts generally have three compositionally and texturally distinct zones; an example of the compositional variation in one grain is shown Fig. 2a. The innermost core is nearly pure albite ($An_{0.2}$ to $An_{1.1}$), next is an outer core of albite with compositions between $An_{1.5}$ and $An_{3.9}$, surrounded by a sharp compositional and optical discontinuity, followed by outer rim with compositions between $An_{21.5}$ and $An_{30.7}$. In some grains the rims and outer cores contain inclusion trains that are sigmoidal in pattern, suggesting possible rotation during growth. The overall compositional zoning of the grains is concentric and the anorthite content increases from core to rim with a reversal in trend near the edges. The optical and compositional discontinuity present in all porphyroblasts is parallel to the concentric zoning pattern.

In the V_b vein, plagioclase has calcic cores with zoning toward less calcic rims (Fig. 2b). Several grains in JR-5-B show increasing anorthite content from cores of about An_{27} to about An_{34} a few tenths of a millimeter away, followed by a reversal and a trend of decreasing anorthite to rims of about An_{15}. Some grains have thin albite rims, $An_{1.6}$ to $An_{2.1}$, separated from grain interiors by optical discontinuities. Such albite rims are found on grains from the center of the vein, but not on grains from the vein edge.

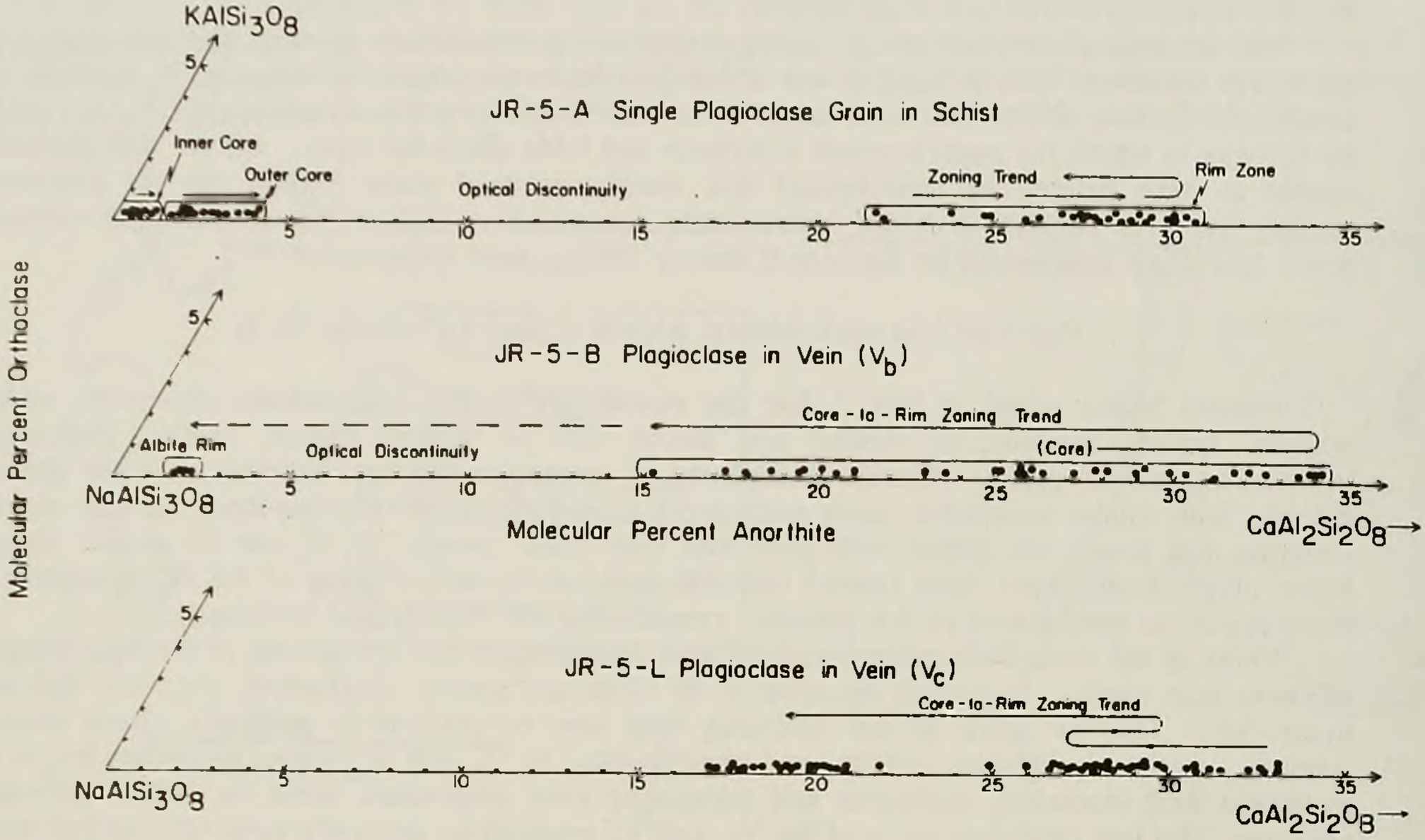

Figure 2. Compositional plots of plagioclase of (a) a single schist porphyroblast in JR-5-A, (b) all analyzed grains in JR-5-B from a V_b vein, and (c) all analyzed grains in JR-5-L from a V_c vein.

Chlorite in both the schist and vein of JR-5-A has a wide compositional range. The host rock chlorite points fall into two compositional groups (Fig. 3a) that correspond to two different textural settings. Points designated as M_a are from small chlorite inclusions within the inner albite cores of the plagioclase porphyroblasts. The compositions shown as M_b come from chlorite grains in the matrix around plagioclase porphyroblasts and from included chlorite in the outer albite cores and oligoclase-andesine rims. Analyzed points in V_b vein chlorite (Fig. 3b) have extensive compositional overlap with M_b chlorite in the schist.

Relatively coarse grains of major minerals are present in many samples along the host-vein interface. Coarse mineral growth or recrystallization that occurred in the original host rock immediately adjacent to the tension fracture is termed here to be in the "vein margin". Some of the vein margin grains also partially extend into the tension fracture. Vein margin growth is texturally different than growth in what is termed here a vein "border zone". Border zones are concentrations of certain minerals (variable from case to case) that have grown within the tension fracture and abut the host-vein interface. It is common for Al-rich minerals to be concentrated in border zones. A moderately well-developed border zone is present in the V_c vein discussed at Stop 1. Coarse euhedral to subhedral plagioclase grains, with minor chlorite, are concentrated in a relatively narrow zone along the host-vein interface. Many veins do not have any border zone developed and in those that do the zone is not necessarily developed everywhere along the host-vein interface. The presence of minor minerals like zircon, graphite, and others in the host rock and their absence in the vein help to locate the host-vein interface.

The most likely mechanism for the zoning in the schist plagioclase was the progressive reaction of epidote with plagioclase to make more Ca-rich plagioclase over a period of slowly increasing metamorphic grade. The apparent change in grade was probably due to increasing T (with presumably increasing P_{load}), but the same effect could have been produced by decreasing

TABLE 1. Structural elements in the study area
(equivalent elements line up horizontally)

A. Ordovician and Cambrian rocks (north-central Vermont)				B. Silurian and Devonian rocks (northeastern Vermont)				C. Structural element designation of Anderson (1977a)				
S-surfaces	Folds	Veins	Mineral growth	S-surfaces	Folds	Veins	Mineral growth	S-surfaces	Folds	Veins	Mineral growth	Approx. age, m.y.
S_a	--	V_a	M_a	--	--	--	--	OS_a	OF_a	OV_a	OM_a	
S_b	F_b (E-W)	V_b	M_b	--	--	--	--	OS_b	OF_b	OV_b	OM_b	440-460 *
S_c	F_c (N-S)	V_c	M_c	S_a	F_a (N-S to NNE-SSW)	V_a	M_a	DS_a	DF_a	DV_a	DM_a	380 **
S_d	F_d (N-S to NNE-SSW)	--	M_d (minor)	S_b	F_b (NNE-SSW)	--	M_b	DS_b	DF_b	--	DM_b	
--	--	V_e	M_e	--	--	V_c	M_c	--	--	DV_c	DM_c	350-360 ***
--	--	--	--	--	F_d (NNE-SSW)	--	--	--	DF_d	--	--	

* Lanphere and Albee (1974) and unpubl. data of M. Lanphere
** Estimate of Laird and Albee (1981b) for D1 using using data of Naylor (1971) and Harper (1968) and unpubl. data of M. Lanphere
*** Unpubl. data of M. Lanphere on Vc veins

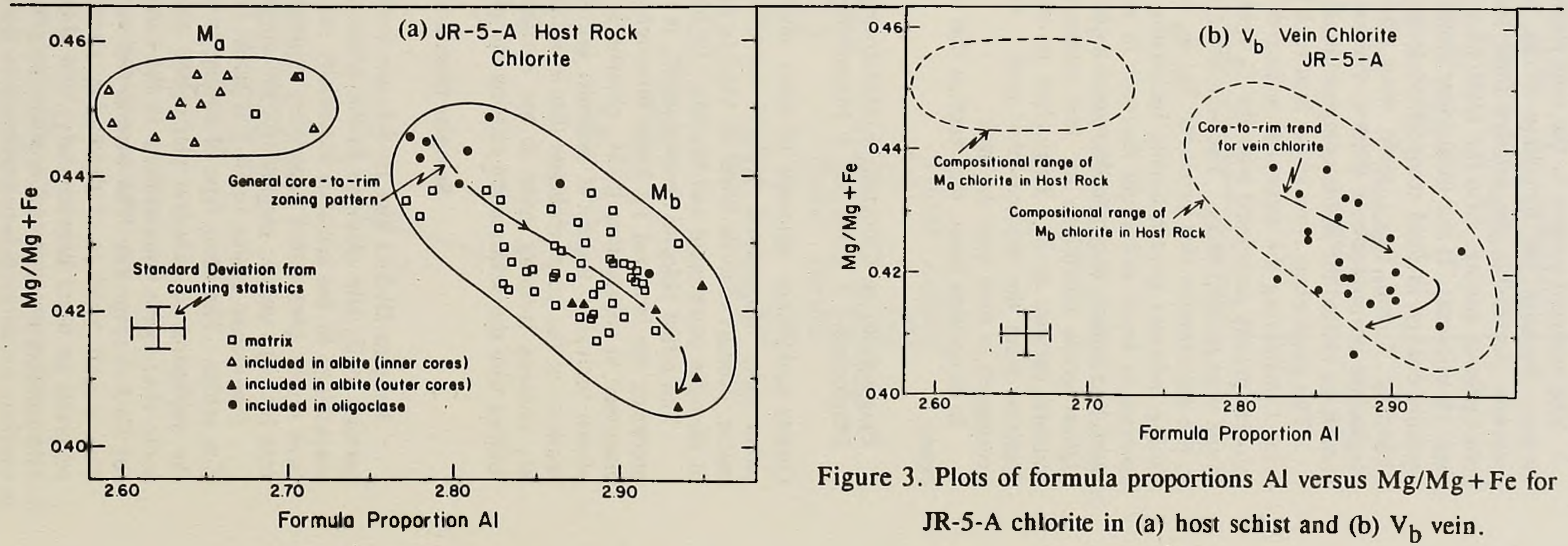

Figure 3. Plots of formula proportions Al versus Mg/Mg+Fe for JR-5-A chlorite in (a) host schist and (b) V_b vein.

P_{H2O} either by decreasing the total fluid pressure or by changing the fluid composition. Calcite might also have been a reactant, in which case P_{CO2} would have been important. Several reactions generally similar to those that may have occurred in JR-5-A have been discussed by Crawford (1966).

The reversed pattern in the vein plagioclase indicates that grade was decreasing as the V_b vein formed. Because the formation of V_b veins in tension fractures required high relative fluid pressure, decreasing the relative fluid pressure is not a possible mechanism for the plagioclase compositional zoning. Also the veins have abundant small fluid inclusions (diameters generally less than 15 microns). If the plagioclase zoning was due to changing fluid composition, then the exact opposite change in fluid composition from that for the schist would have been needed for the vein. Changing T and P_{total} seem most likely. The optical and compositional discontinuities in plagioclase porphyroblasts seem to represent the peristerite gap, encountered as changing physical conditions shifted the stable composition of reaction products.

The plagioclase rims in the host rock are compositionally similar to plagioclase cores in the V_b vein. Considering the structural setting of the mineral growth in the schist and in the vein, schist mineral growth associated with the S_b schistosity probably began to form before the mineral growth in the vein parallel to S_b. The vein has no evidence of post-formation recrystallization or strain due to the deformation that produced S_b; S_b began to form before the V_b vein. The schist plagioclase zoning indicates growth during increasing grade up to the "peak" of the metamorphic event. The reversal in trend and slight decrease in anorthite content as the rims are approached may indicate some late growth as grade decreased from the metamorphic peak. When the system approached the highest grade conditions for this metamorphic event, the V_b vein began to form in a tension fracture parallel to S_b. Plagioclase in the vein grew as the grade conditions reached and then declined from the metamorphic peak. Growth of vein and schist plagioclase probably partially overlapped in time near the peak.

In simplified form, the reaction that accompanied mineral growth in JR-5-A schist might have been:

$$\text{Plagioclase}_1 + \text{Chlorite}_1 + \text{Muscovite}_1 + \text{Epidote} \rightarrow \text{Plagioclase}_2 + \text{Chlorite}_2 + \text{Muscovite}_2 + H_2O$$

Quartz and minor amounts of other minerals needed to balance the reaction could be added to either side. Compared to their respective reactant compositions, product plagioclase was more calcic, product chlorite lower in Mg/Mg+Fe and higher in Al/Al+Si, and product muscovite lower in phengite component and Mg/Mg+Fe for the period of prograde growth.

The schist chlorite denoted as M_a is interpreted as having been formed with the S_a schistosity, predating the isoclinal F_b folds, although evidence available from other outcrops would have to be discussed to substantiate it. M_a chlorite is included in the inner zones of plagioclase porphyroblasts where inclusion trains, if present, are straight, whereas the inclusions of M_b chlorite are in portions of the porphyroblasts that in some cases have sigmoidal trains. This is compatible with the M_a chlorite forming prior to the isoclinal F_b folding and the M_b chlorite forming during F_b folding with the deformation causing the plagioclase porphyroblasts to rotate as they grew.

Samples from a V_c vein - JR-5-G and JR-5-L

Samples JR-5-G and JR-5-L are from the contact between schist and a V_c vein. The vein is parallel to S_c slip cleavage in the schist and lies in the axial region of a small F_c synform. The assemblage in the schist is essentially the same as that for JR-5-A except that JR-5-G and JR-5-L have minor garnet that is partially replaced by chlorite and muscovite. The assemblage in the V_c vein includes quartz, plagioclase, muscovite, chlorite, calcite, apatite, and pyrrhotite.

Plagioclase grains in JR-5-G schist have more complex compositional zoning than those in JR-5-A schist. The same type of zoning is found in sample JR-5-I, described later. In the V_c vein, the subhedral to euhedral plagioclase grains are concentrically zoned from calcic cores to more sodic rims, with compositions in the range $An_{33.1}$ to $An_{14.8}$ for JR-5-G and $An_{33.0}$ to $An_{16.9}$ for JR-5-L (Fig. 2c). The core-to-rim zoning trends in plagioclase are the same in both samples. The overall trend is of decreasing anorthite content from the calcic cores, but with two small reversals in trend between An_{27} and about An_{30}. Albite has not been found in the analyzed V_c vein samples except as a late alteration product.

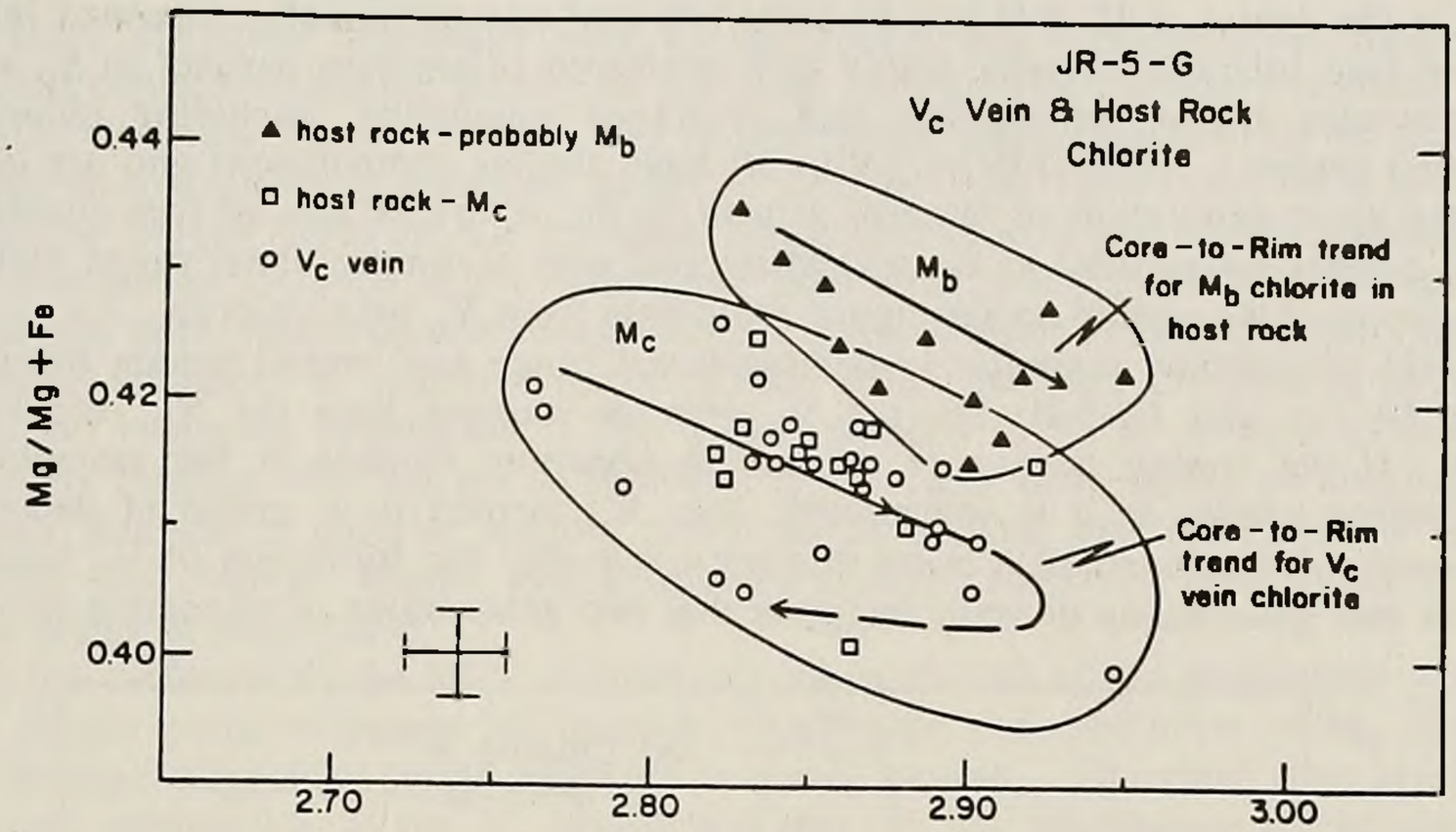

Figure 4. Plot of formula proportions Al versus Mg/Mg+Fe for chlorite in V_c vein and schist of JR-5-G.

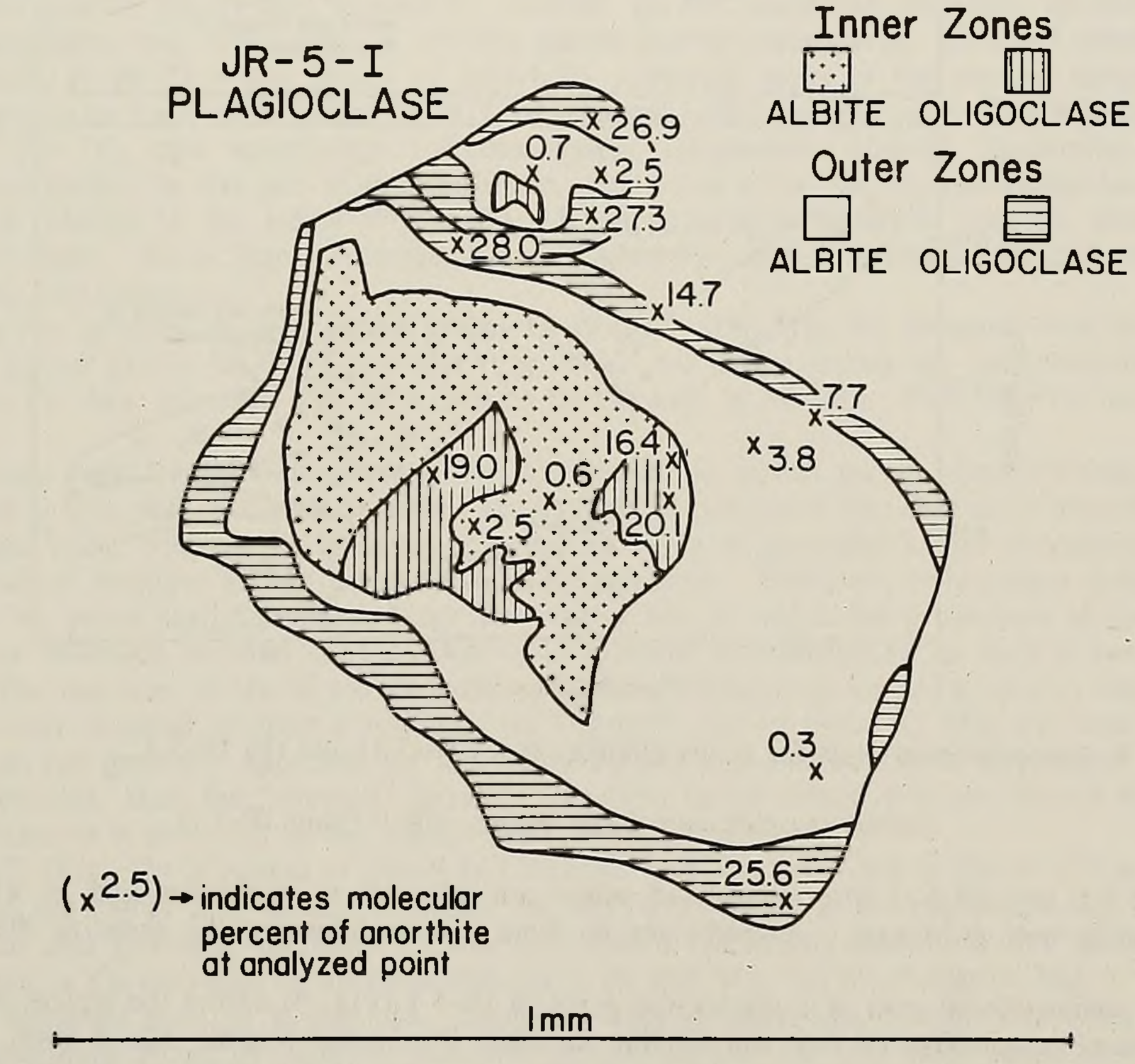

Figure 5. Compositional map of plagioclase grain in JR-5-I schist. Grain map taken from electron beam scanning image of Ca distribution, augmented with conventional quantitative analyses at points indicated with "x".

Chlorite in the schist of JR-5-G can be texturally and compositionally separated into two types (Fig. 4). One type includes chlorite grains with preferred orientation parallel to S_c slip cleavage plus some otherwise similar grains that lack preferred orientation, including chlorite that has partially replaced garnet. These chlorite grains all have similar compositions and are interpreted as representing the same generation of mineral growth in the schist. A second type consists of grains with preferred orientation parallel to S_b schistosity and with a compositional range that is different from the first group. Also plotted on the figure are points from V_c vein chlorite.

The V_c vein plagioclase is similar in compositional range and overall zoning trend to V_b vein plagioclase in JR-5-A and JR-5-B, but the V_c vein is younger than the V_b vein by structural superposition. If the zoning pattern of decreasing anorthite content in the assemblage present indicates decreasing grade, as it is interpreted, then V_c formed in a period of decreasing grade following the peak of a metamorphic event that occurred after the formation of V_b veins. Presence of oligoclase in two generations of veins suggests that two generations of oligoclase might be in the schist.

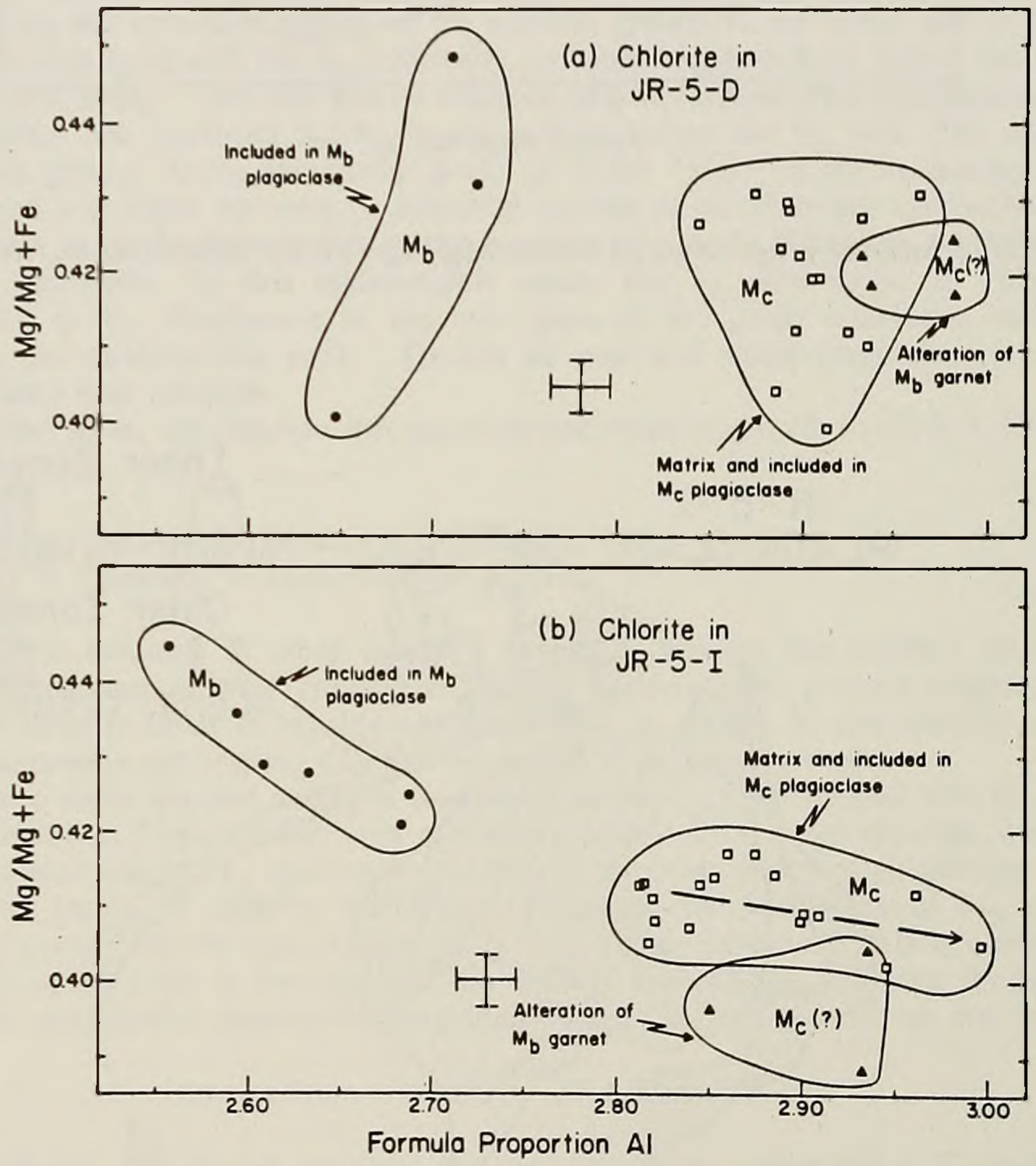

Figure 6. Compositional plots for schist chlorite in (a) JR-5-D and (b) JR-5-I.

Schist samples away from veins - JR-5-I and JR-5-D

JR-5-I and JR-5-D are samples of schist not adjacent to any veins and in which S_c slip cleavage is well developed. Assemblages in these two samples are the same as that in JR-5-G schist.

A compositional map of a plagioclase grain in JR-5-I (Fig. 5) shows the typical compositional zonation of plagioclase in this and similar samples. The mapped grain has a core, cloudy with inclusions of very fine-grained graphite and other minerals, that consists of an area of albite and two areas of oligoclase. The cloudy zone is completely surrounded by a zone of clear, graphite inclusion-free albite, in turn surrounded by an outer zone of clear oligoclase. The zoning pattern in the outer, clear zones is increasing anorthite content from core to rim. The clear albite zone is

separated from the clear oligoclase zone by an optical and compositional discontinuity that is parallel to the concentric zoning pattern in the clear zones. The boundary between the clear albite and cloudy inner zones is not parallel to any compositional zoning patterns of the cloudy interior.

Figures 6a and 6b show analyzed points in chlorite from JR-5-I and JR-5-D. Chlorite grains included in the cloudy cores of the complex plagioclase grains are compositionally distinct from chlorite grains grains included in the clear outer zones. Very few grains in the matrix of the schist of either sample have preferred orientation parallel to S_b schistosity, but analyzed grains that do are compositionally identical to matrix chlorite grains with preferred orientation parallel to S_c slip cleavage or no preferred orientation. The grains parallel to S_c or without preferred orientation compositionally overlap with the grains included in the clear outer zones of the plagioclase grains. Also in both samples is chlorite without preferred orientation that has partially replaced garnet; analyses from this chlorite, shown with a separate symbol, plot very close to the chlorite included in the clear zones of plagioclase.

Using the evidence all the JR-5 samples, an interpretation of the plagioclase grain in Figure 5 is that the cloudy cores represent M_b growth, or perhaps a combination of M_a albite growth and M_b albite through oligoclase (sodic andesine in some) growth. The clear rims are M_c growth and have the same relationship to the V_c plagioclase that the M_b plagioclase in the simple plagioclase grains of JR-5-A have to M_b growth in the V_b vein. Two generations of oligoclase to sodic andesine are present in the schist and similar plagioclase with reversed zoning patterns is found in two distinctly different generations of veins.

Stop 2 (location JR-73)

Discussed below are analyzed garnet in two samples from Stop 2, a V_b vein (JR-73-B) and schist (JR-73-A) about 1 meter from the V_b vein. Typical pelitic schist at JR-73 has an assemblage that includes quartz, plagioclase, muscovite, chlorite, garnet, magnetite, ilmenite, epidote, pyrite, apatite, tourmaline, and zircon with or without calcite and/or chalcopyrite. Included within garnet porphyroblasts of JR-73-A are grains of chloritoid, although none of the studied samples have chloritoid grains in the matrix. Schist in JR-73-B adjacent to the V_b vein lacks chloritoid inclusions in garnet. The V_b vein assemblage includes quartz, plagioclase, chlorite, muscovite, calcite, ilmenite, and garnet. In this part of the study area, only veins of the the V_b generation have garnet within them. Garnet in the schist is probably M_b in generation based on textural, assemblage, chemical evidence. As at Stop 1, retrogradation of garnet is most extensive in samples with well-developed S_c slip cleavage.

Rim-to-rim profiles of vein garnet grains in JR-73-B (Fig. 7a) are different than rim-to-rim profiles of garnet grains in JR-73-A schist (Fig. 7b). All of the grains are concentrically zoned with respect Fe, Mn, Mg, and Ca) as illustrated by the map of Mn/Mn+Fe+Mg+Ca for grain A (Fig. 8).

The inner parts of the vein garnet grains are similar to typical garnet porphyroblasts in host pelitic schist in this part of the study area. Mn is high in the center and decreases toward the rim in this center zone, whereas Fe increases core-to-rim. Mg is generally in low concentration and shows a gradual increase as Mn decreases and Fe increases. However, only garnet grains in or adjacent to V_b veins have the sharp, inner reversal of Mn in which the proportion of spessartine increases by as much as 10% of the total solid solution over distances of only a few tens of microns. The increase in Mn is accompanied by a sharp decrease in Fe and a smaller decrease in Mg. The outer reversal involves a return to the "normal" zoning trend for Mn, Fe, and Mg, but the values do not generally approach the maximum Fe and Mg and minimum Mn values found at the inner reversal. How the "average" trend of Ca might be correlated with the overall trends for the other elements is obscured by the small scale Ca variations.

Grain D (Fig. 7b) is typical of garnet in Underhill and Hazens Notch schist in this area. Mn is highest in the center and decreases toward the rim, whereas Fe is the opposite. Mg is low in concentration and gradually increases as Mn decreases. Ca zoning has an erratic pattern, with sharp changes in Ca mirrored by opposite changes in Fe and Mn, but no change in Mg.

Other minerals such as plagioclase, chlorite, muscovite, ilmenite, calcite, and chloritoid are also compositionally zoned in these two samples. Besides garnet, the only other major mineral with significant variation in Ca is plagioclase, which has zoning patterns similar to those for M_b schist and vein plagioclase at Stop 1. Calcite grains are zoned with respect to Fe-Mg-Mn substitution for Ca, but the range of Ca variation is limited. Epidote grains are zoned with respect to Fe and Al but not Ca, except in small REE-rich cores in some grains where Ca varies due to the REE substitution

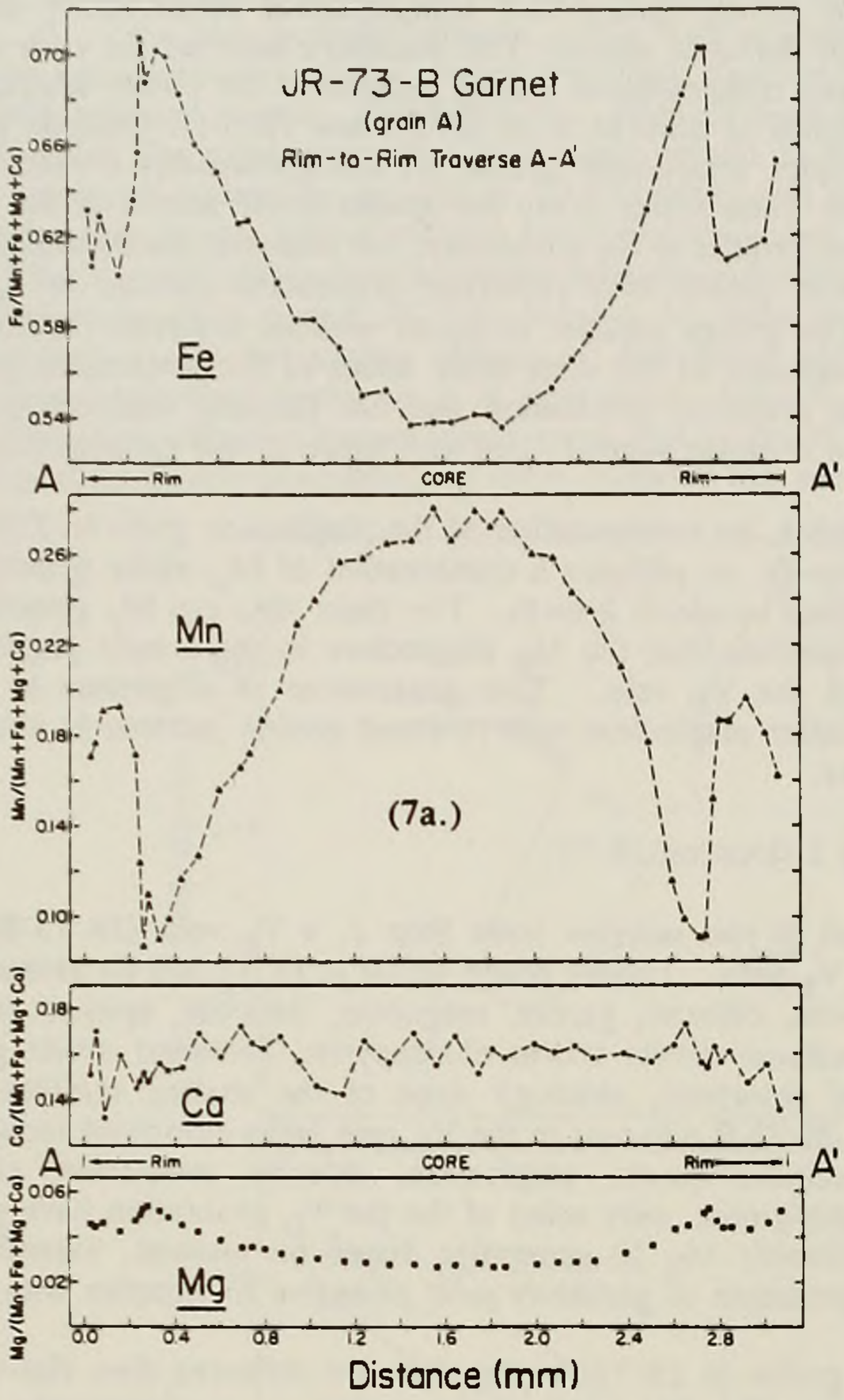

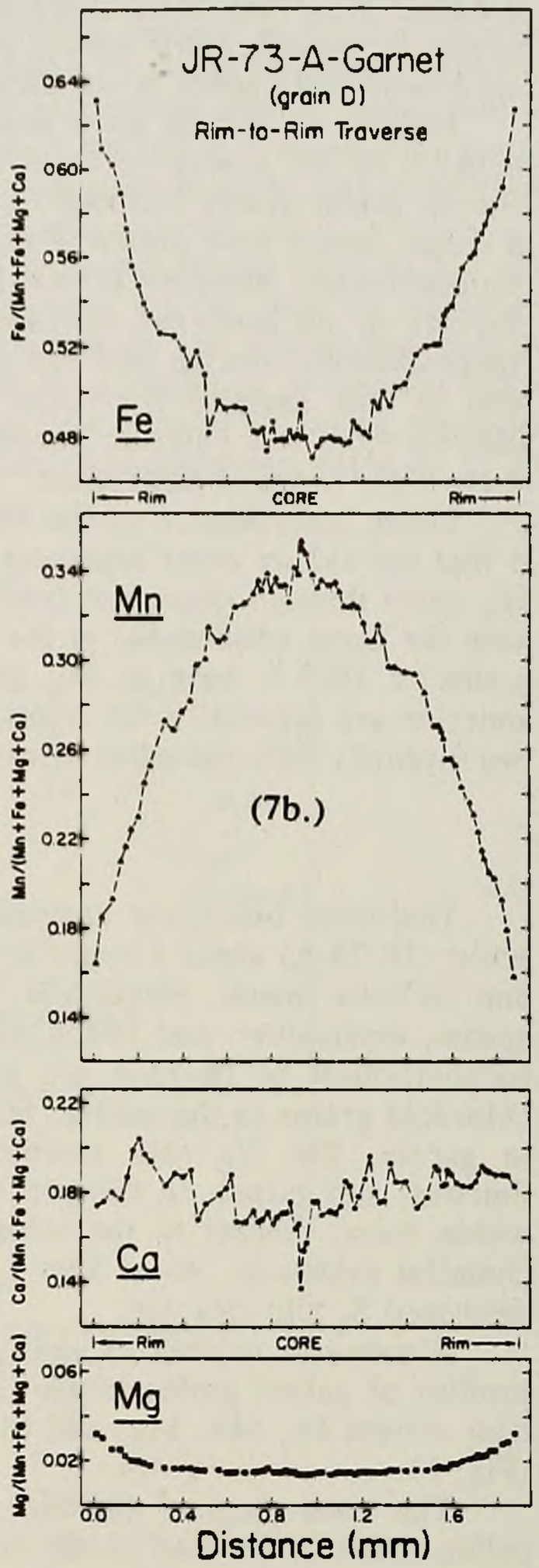

Figure 7. Compositional profiles of garnet grains.
(a) Grain A, euhedral grain in V_b vein of JR-73-B.
(b) Grain D, subhedral porphyroblast in JR-73-A schist.

Figure 8. Compositional map of garnet grain in V_b vein of JR-73-B, contoured with respect to Mn/Mn+Fe+Mg+Ca. Traverse in Fig. 7a is shown as A-A'.

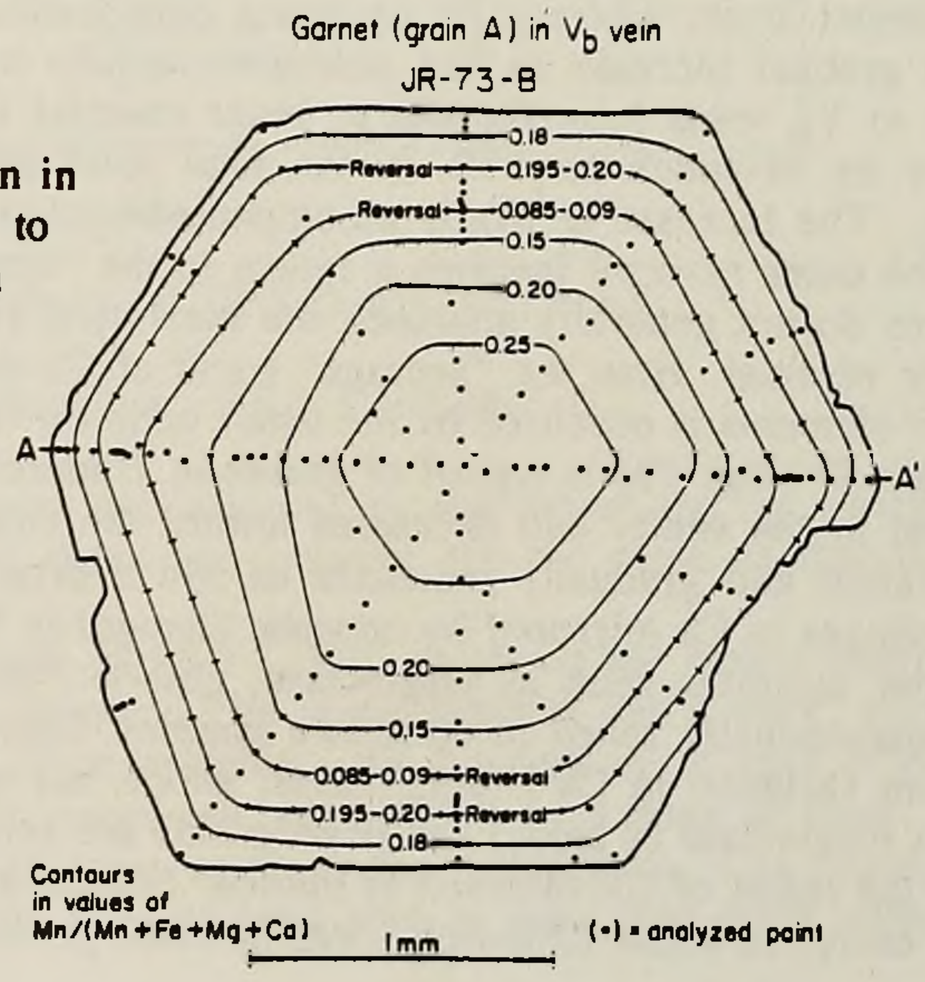

(REE-rich cores have up to 7 wt. % $Y_2O_3+Ce_2O_3+La_2O_3+Nd_2O_3$). Mn-bearing phases other than garnet are ilmenite, chlorite, calcite, and chloritoid.

Textural evidence indicates chloritoid was once present in the matrix of some of the schist but was removed by reaction. Chloritoid grains included in garnet have Mg/Mg+Fe values in the range 0.08 to 0.11 and MnO contents in the range 1.47 to 1.87 wt. %. Ilmenite grains in JR-73-A have MnO contents in the range 1.69 to 2.59%, but there is no textural evidence of substantial reaction of ilmenite. V_b vein calcite have MnO contents in the range 0.24-1.67%.

JR-73-A schist and JR-73-B vein chlorite grains have MnO contents of 0.27-0.51 and 0.24-0.45%, respectively, along with wide compositional ranges with regard to Mg, Fe, Si, and Al. Mn variation in vein chlorite is grossly similar to that in the vein garnet, except much lower concentrations are involved. Cores tend to be high in Mn, which decreases toward the rims, then increases and, on the rims of some grains, decreases again.

Neglecting the fine-scale details, the best explanation for the zoning trends of garnet and other M_b minerals in the schist and V_b vein of JR-73 is shifting equilibrium partitioning among phases as conditions first increased in grade, then decreased. The vein and schist M_b growth probably overlapped in time, but the schist growth began first and the last growth was in the V_b vein. The relatively late breakdown of Mn-bearing chloritoid in the schist may help explain the Mn "spike" in vein garnet and possible smaller counterpart in vein chlorite.

Stowe amphibolite in the Worcester Mountains - Stops 5 & 9

Exposed at both locations are amphibolites metamorphosed to at least garnet grade and then later subjected to retrogradation at chlorite to biotite grade. This is typical of rocks of the Worcester Mountains and in much of the area the higher-grade assemblages have been badly obscured or completely eliminated by retrograde events. The extent of preservation of the higher-grade assemblages and the character of the deformation elements in the Worcester Mountains tend to vary with rock types. Equivalent deformational elements in amphibolite and pelitic schist can have different styles or degrees of development. In general, the amphibolite is less deformed and less affected by the late retrograde metamorphism than pelitic schist.

The age of coarse muscovite from a V_b vein in the Worcester Mountains has been determined by Lanphere and Albee (1974) to be 439 m. y. using ^{40}Ar-^{39}Ar methods (the vein was shown to the author in the field by A. Albee). Other primary minerals in the vein are kyanite, garnet, and biotite, now mostly altered. Fine-grained muscovite, pseudomorphous after kyanite, in schist adjacent to the V_b vein was determined by Lanphere and Albee to be 358 m. y. in age. They also analyzed hornblende from Stowe amphibolite at another location in the Worcester Mountains and it had an age of 457 m. y.

Stop 5 (similar to JR-188, 2 miles SE on Mt. Hunger)

Sample JR-188-A is amphibolite with a small V_b vein, parallel to S_b schistosity, and a several small V_c veins parallel to S_c fracture cleavage. The amphibolite assemblage includes hornblende, plagioclase, epidote, quartz, chlorite, biotite, rutile, sphene, muscovite, and apatite. Also present is actinolite after hornblende and some of the actinolite is in bands parallel to S_c that cut across hornblende grains. Some of the chlorite, biotite, epidote, and perhaps all of the sphene are retrograde minerals formed by reaction of hornblende that has preferred orientation parallel to S_b. The V_c veins have actinolite, plagioclase, quartz, epidote, sphene, and chlorite. The V_c veins are similar to those at Stop 9. The V_b vein has amphibole grains with euhedral hornblende cores overgrown by euhedral actinolite rims. This actinolite is texturally and compositionally different (with lower Mg/Mg+Fe values) from that in V_c veins and from the actinolite formed at the expense of hornblende in the host rock. The hornblende interiors of V_b vein amphibole grains are separated from the actinolite rims by sharp optical and compositional discontinuities not unlike the discontinuities described for plagioclase.

Compositional profiles from several core-to-rim traverses across V_b vein amphibole and host rock hornblende (Fig. 9) illustrate the zoning patterns in these two amphibole types. Hornblende interiors of vein amphibole are compositionally similar to host rock amphibole, but the actinolite rims of the vein amphibole are very different.

V_b vein amphibole is similar in a general way to V_b vein plagioclase from JR-5 and JR-73. It grew as grade conditions were changing and the last growth occurred as grade was decreasing. (The compositional variation of amphibole with grade in amphibolites with the same assemblage as

JR-188-A has been discussed by Laird and Albee, 1981b.) Interiors of vein amphibole grains formed at the highest grade and their growth may have overlapped in time with the last growth of M_b host rock hornblende. Amphibole in both the V_b vein and host rock was growing when the peak of the M_b-forming event was attained. As grade conditions declined from the peak, the host rock amphibole ceased to grow but the vein amphibole continued to form in an environment suitable for maintaining euhedral grain shapes. The grade decreased enough for actinolite to become the stable amphibole composition. The discontinuity present in V_b vein amphibole grains could represent either a hiatus in growth or a miscibility gap encountered as conditions changed over time.

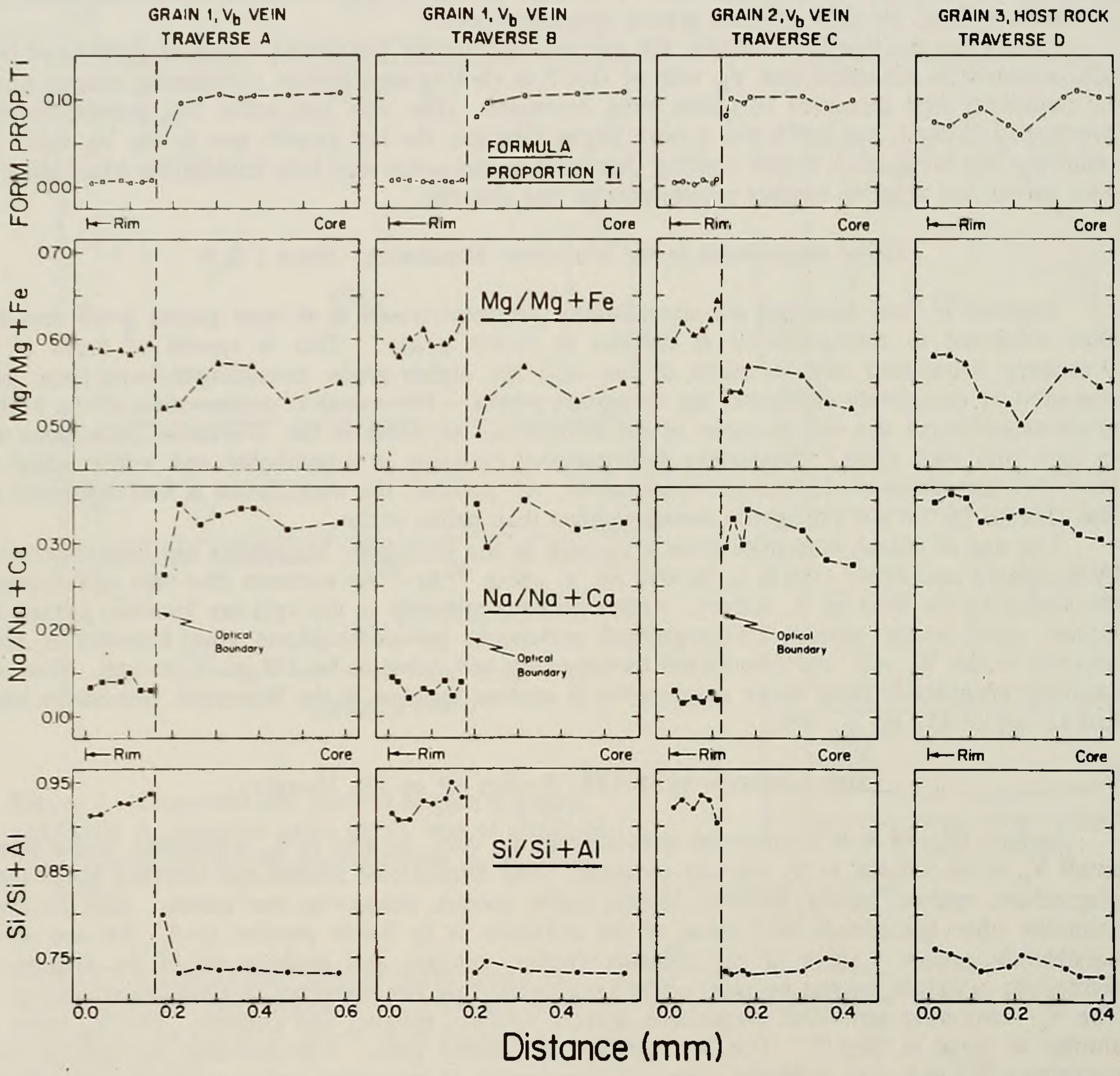

Figure 9. Core-to-rim compositional profiles with respect to Si/Si+Al, Na/Na+Ca, Mg/Mg+Fe, and formula proportions Ti for two amphibole grains in V_b vein and one amphibole grain in host amphibolite, sample JR-188-A.

Stop 9 (location JR-66)

Sample JR-66-F is from a V_c vein parallel to S_c fracture cleavage in Stowe amphibolite. The exposed vein is lens-shaped, 30 cm long and 10 cm at its maximum width. The vein assemblage includes quartz, plagioclase, actinolitic amphibole, chlorite, biotite, microcline, epidote, hematite, magnetite, sphene, and calcite. The host amphibolite has a higher-grade assemblage that was

strongly overpinted by at least one retrograde event. The pre-retrograde assemblage of the host rock includes hornblende, plagioclase, epidote, chlorite, quartz, magnetite, and ilmenite. The host rock retrograde assemblage is the same as the vein primary assemblage, except that in the former microcline is lacking and none of the magnetite is of obvious retrograde origin.

Developed along the host-vein interface of the V_c vein is a 1-2 mm wide border zone, present along most but not all of the examined area of the interface. A zone of chlorite with preferred orientation parallel to the host-vein interface is developed adjacent to the interface. Toward the vein interior, the next zone is one of intergrown chlorite and biotite with the same preferred orientation as the chlorite zone. An innermost zone of biotite with lens-shaped grains of microcline is sporadically developed. Locally developed between the chlorite-biotite or biotite zone and the quartz-rich vein interior is a monomineralic zone of hematite.

Euhedral amphibole grains are distributed throughout all parts of the border zone except the hematite zone. Similar euhedral amphibole grains are in the vein interior. More than half of the amphibole grains in the border zone have preferred orientation with their direction of elongation perpendicular to the host-vein interface. This suggests that some mechanism other than directed stress was responsible for the preferred orientation in the vein border zone. None of the minerals in the vein interior have preferred orientation.

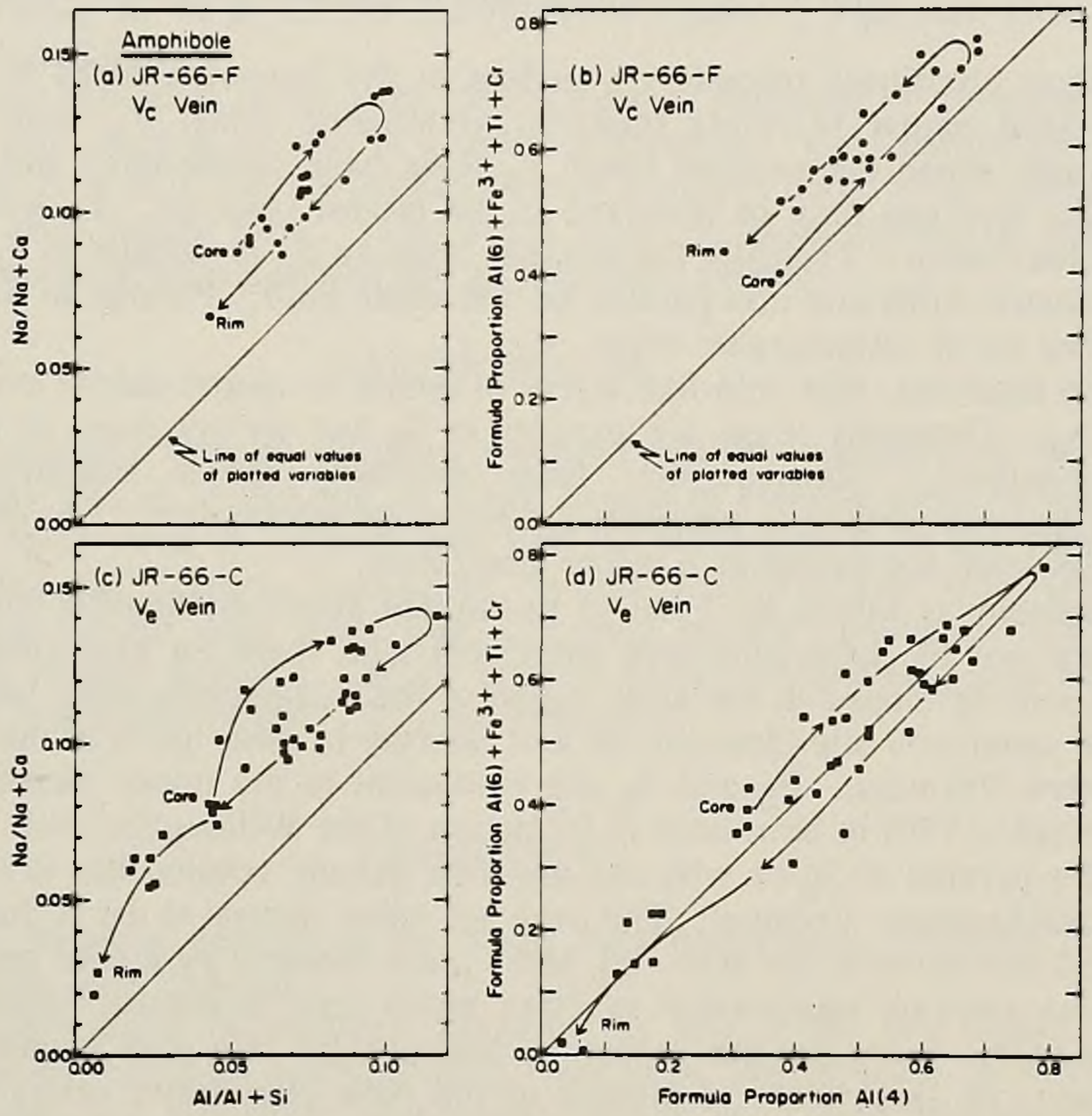

Figure 10. Plots of Al/Al+Si versus Na/Na+Ca and Al(4) versus $Al(6)+Fe^{3+}+Ti+Cr$ for Ca-amphibole in JR-66 samples. (a, b) JR-66-F V_c vein. (c, d) JR-66-C V_e vein.

Typical amphibole grains in the border zone are concentrically zoned with respect to composition. The core-to-rim variation trend (Fig. 10a, b) starts with actinolitic cores, progressively becomes more hornblende-rich, reverses in trend and finally zones out to actinolitic rims with compositions very much like the core compositions. No discontinuities, optical or compositional, are found in the vein amphibole grains. Comparing these compositions to amphibole compositions discussed by Laird and Albee (1981b), the V_c amphibole formed at biotite-grade conditions under an intermediate relative pressure.

Within the host amphibolite of JR-66-F are three compositional ranges of amphibole. Cores of dark amphibole grains have compositions similar to the host rock amphibole of JR-188-A and V_b vein hornblende cores. The hornblende cores are overgrown by more actinolitic amphibole that is similar to the actinolitic rims of the V_b vein amphibole in JR-188-A. A third type of amphibole is present as irregular patches of actinolite that replaces the first two types. This third type compositionally overlaps with the V_c amphibole of JR-66-F. Other retrograde products such as

fine-grained chlorite and biotite are closely associated with the patchy actinolite and they overlap compositionally with their counterparts in the V_c vein as well.

Sample JR-66-C is from a V_e vein that crosscuts S_c fracture cleavage in Stowe amphibolite. The vein assemblage includes albite, calcite, actinolite-tremolite, chlorite, biotite, epidote, magnetite, hematite, sphene, apatite, and minor quartz. This vein does not have a well-developed border zone. Amphibole grains are euhedral with core-to-rim compositional trends for concentrically zoned grains as shown in Fig. 10c, d. The cores are similar to cores of V_c vein amphibole in JR-66-F. The initial trend is increasing Al(4), A-site Na, and $Al(6)+Fe^{3+}+Ti+Cr$ toward more hornblende-rich compositions. Then a reversal in trend occurs and the grains are zoned out to tremolitic rims with very low values of Al and Na.

Although the V_c and V_e veins at Stop 9 both contain assemblages that are the same as the retrograde assemblage found in the host assemblage, the two vein types are structurally distinct in age. Therefore, two generations of retrograde mineral growth (M_c and M_e) can be postulated. Both veins began to grow as grade conditions were increasing in their respective metamorphic events and continued to form as the peak was attained and as conditions declined to lower grade. Growth in the V_e vein continued to lower grade than that attained by the V_c vein.

Stop 10 (a brief look into the Siluro-Devonian units)

The oldest prominent secondary s-surface in the Devonian rocks of this area is a schistosity, S_a, that is axial planar to rarely observed asymmetric folds, F_a, with N-S to NNE-SSW axial trends. In many cases the smallest order F_a folds have wavelengths and amplitudes of sufficiently large size that they can only be observed in the largest roadcuts. F_a folds can be seen at Stop 10 on careful observation. Typically the original layering S_0 is parallel to F_a axial planes on one limb of the asymmetric folds and non-parallel on the other limb. Parallel to S_a schistosity is a generally well-developed set of metamorphic veins, V_a.

At some locations, thin vein-like layers of quartz or quartz-calcite are present that appear to be older than S_a. Generally these are parallel to S_0 but do not seem to be related to a prominent secondary s-surface. Because they have invariably simple assemblages and have no clear relationship to other structural elements produced by deformation or to major metamorphic mineral growth, these veins are treated as a minor generation.

S_a schistosity is folded by a set of prominent small asymmetric folds, with NNE-SSW axial trends. These are F_b folds and have associated with them an axial-planar s-surface, S_b. S_b is particularly well developed in the axial region of the Willoughby arch, where it is a schistosity, but it is either a prominent slip cleavage or a schistosity in other parts of the post-Ordovician sequence of northeastern Vermont. F_b and S_b are equivalent to the minor elements interpreted by Dennis (1956) and Hall (1959) to be related to formation of the Willoughby arch.

No veins parallel to S_b or with any apparent genetic relationship to F_b have been found by the author in northeastern Vermont. The lack of veins seems to be a fundamental feature of this generation of structures in the area. S_b and F_b are crosscut by a later generation of veins, V_c. V_c veins have no obvious relationship to other small-scale structural elements but do have mineral assemblages within them that are subsets of assemblages of a post-S_b mineral growth generation in the host rocks. In areas close to plutons of the New Hampshire series in northeastern Vermont, this late mineral growth generation (M_c) attained grade as high as sillimanite-muscovite. Characteristic of M_c is the random orientation of minerals that in an environment of directed stress would typically have preferred orientation. A few V_c veins have been found that crosscut semiconcordant sheets of granitic rock associated with the New Hampshire series. However, the M_c mineral growth generation has such a close spatial relationship with the plutons with regard to metamorphic grade that the veins were probably formed about the same time as the intrusion and solidification of some of the plutons.

A late generation of open, asymmetric folds with NNE-SSW axial trends and upright axial planes deform the V_c veins. These folds, F_d, are difficult to recognize without the V_c veins as markers, although they also gently deform S_c schistosity or slip cleavage. No s-surface or veins related to F_d have been found. The only other significant generation of structural features found in this part of the study area, except for minor veins, is a locally developed set of open, asymmetric folds with E-W axial trends, upright axial planes, and, where present at all, a poorly-developed axial-plane slip cleavage. These E-W folds are younger than F_a, older than F_d, and may be younger than F_b, although the interference structures (basin-and-dome structures formed on S_a surfaces) produced by the N-S F_b folds and these E-W folds are such that the superposition

relationships are ambiguous; an excellent example is at Stop 10. The E-W folds are designated F_{b+1}, have no associated veins, and are not apparently associated with any substantial mineral growth in the host rock. The structural sequence (excluding F_{b+1}) in Siluro-Devonian units is summarized in part B of Table 1. The interpreted correlation (one which agrees with the scarce age data) across the unconformity between the Cambro-Ordovician and Siluro-Devonian is shown in Table 1, Part C.

Conclusions

Metamorphic veins were formed during four of the five major metamorphic events that occurred during the Taconic and Acadian Orogenies in northern Vermont. The compositional zoning patterns of key minerals in the veins and surrounding host rocks recorded the effects of changing physical and/or chemical conditions during each event. Most of the host rock mineral growth occurred as grade was increasing to the metamorphic peak of each event, in some cases with minor continued growth as grade declined from the peak. Substantial mineral growth in the veins occurred as grade was decreasing from the peak, with varying amounts of early growth overlapping with the prograde host rock mineral growth. By the methods used, each event with associated veins is shown to be a distinct metamorphic "pulse", separated from other events by periods of low-grade conditions.

The timing of vein initiation varied from case to case as indicated by the variation in amount of overlap of host and vein mineral growth of a given generation. The distribution of stress and the relative fluid pressure in a rock volume probably were principal controlling factors that determined where and when a vein would form. The veins grew by precipitation of material in tension fractures and replacement of host rock was not an important process.

Acknowledgements

A study of metamorphic veins in northern Vermont was first suggested to the author by Arden L. Albee. Discussions with A. Albee and J. Laird helped in refining some of the ideas presented. The portion of the study done at Caltech was part of the author's Ph.D. dissertation and was supported by the National Science Foundation, grants DES75-03416 and GA-12867, both to A. Albee. A portion of the field work was supported by the Geological Society of America, research grants 1745-73 and 1852-74. Work done at SUNY-Binghamton was supported by NSF grants EAR77-23405 and EAR79-04041, both to the author.

REFERENCES

Albee, A. L., 1957, Bedrock geology of the Hyde Park quadrangle, Vermont: U. S. Geological Survey Quadrangle Map GQ-102.

___, 1968, Metamorphic zones in northern Vermont, in Zen, E-an, and others, eds., Studies of Appalachian geology: northern and maritime: New York, Interscience, p. 329-341.

___, 1972, Stratigraphic and structural relationships across the Green Mountain anticlinorium in northcentral Vermont: New England Intercollegiate Geological Conference, Guidebook, p. 179-194.

Anderson, J. R., 1977a, The polymetamorphic sequence in the Paleozoic rocks of northern Vermont: a new approach using metamorphic veins as petrologic and structural markers [Ph.D. thesis]: California Institute of Technology, 656 p.

___, 1977b, Compositional zoning in minerals from low- to medium-grade rocks of northern Vermont [abs.]: Geological Society of America Abstracts with Programs, v. 9, p. 235-236.

___, 1978, Empirical refinement of the peristerite gap: data from metamorphosed Paleozoic rocks of western New England: Geological Society of America Abstracts with Programs, v. 10, p. 359.

___, 1983, Petrology of a portion of the eastern Peninsular Ranges mylonite zone, southern California: Contributions to Mineralogy and Petrology, v. 84, p. 253-271.

Anderson, J. R., and Albee, A. L., 1975, Metamorphic veins as petrologic and structural markers of regional polymetamorphism in northern Vermont [abs.]: Geological Society of America Abstracts with Programs, v. 7, p. 975-976.

Beach, A., 1975, The geometry of en-echelon vein arrays: Tectonophysics, v. 28, p. 245-263.

___, 1977, Vein arrays, hydraulic fractures and pressure solution structures in a deformed flysch sequence: Tectonophysics, v. 40, p. 201-225.

Cady, W. M., 1956, Bedrock geology of the Montpelier quadrangle, Vermont: U. S. Geological Survey Quadrangle Map GQ-79.

___, 1969, Regional tectonic synthesis of northwestern New England and adjacent Quebec: Geological Society of America Memoir 120, 181 p.

Christman, R. A., and Secor, D. T., 1961, Geology of the Camels Hump quadrangle, Vermont: Vermont Geological Survey Bulletin 15, 70 p.

Crawford, M. L., 1966, Composition of plagioclase and associated minerals in some schists from Vermont, USA and South Westland, New Zealand, with inferences about the peristerite solvus: Contributions to Mineralogy and Petrology, v. 13, p. 269-294.

Dennis, J. G., 1956, The geology of the Lyndonville area, Vermont: Vermont Geological Survey Bulletin 8, 98 p.

Etheridge, M. A., 1983, Differential stress magnitudes during regional deformation and metamorphism: upper bound imposed by tensile fracturing: Geology, v. 11, p. 231-234.

Hall, L. M., 1959, The geology of the St. Johnsbury quadrangle, Vermont and New Hampshire: Vermont Geological Survey Bulletin 13, 105 p.

Laird, J., 1977, Phase equilibria in mafic schist and the polymetamorphic history of Vermont [Ph.D. thesis]: California Institute of Technology, 445 p.

Laird, J., and Albee, A. L., 1981a, High-pressure metamorphism in mafic schist from northern Vermont: American Journal of Science, v. 281, p. 97-126.

___, 1981b, Pressure, temperature, and time indicators in mafic schist: their application to reconstructing the polymetamorphic history of Vermont: American Journal of Science, v. 281, p. 127-175.

Lanphere, M. A., and Albee, A. L., 1974, $^{40}Ar/^{39}Ar$ age measurements in the Worcester Mountains: evidence of Ordovician and Devonian metamorphic events in northern Vermont: American Journal of Science, v. 274, p. 545-555.

Secor, D. T., 1969, Mechanics of natural extension fracturing at depth in the Earth's crust: Geological Survey of Canada Paper 68-52, p. 3-48.

White, W. S., and Jahns, R. H., 1950, Structure of central and east-central Vermont: Journal of Geology, v. 58, p. 179-220.

ITINERARY

Assembly point is a picnic area on Route 2 between Middlesex and Waterbury, 2.7 miles east of the junction of Routes 100N and 2 in Waterbury and 2.6 miles west of the Middlesex exit off I-89. Picnic area is on north side of road, with parking on both sides. Meet at 8:30 A.M. Topographic maps: Waterbury, Stowe, and Middlesex 7.5″ quadrangles, Hyde Park, Hardwick, Montpelier, and Barre 15″ quadrangles.

PLEASE: refrain from sampling the veins from which the compositional data come, especially the smaller ones that could be whacked to oblivion.

Mileage

0.0 From assembly point, take Route 2 west (Middlesex quadrangle). Pass through town of Waterbury (Waterbury quadrangle) and continue west.

5.3 Underpass below I-89.

5.8 STOP 1: Large roadcut in pelitic schist of the Hazens Notch formation on right (north) side of road. Park along right side of road, but be careful as room is tight. Pull completely to the right of the solid white line that marks the edge of the travelled surface. Refer to text for detailed discussion of V_b and V_c veins here. (Sample location JR-5.)

6.4 Bolton - Waterbury line.

6.7 STOP 2: Small roadcut on north side of Route 2. Use same care in parking here and at next two stops as at Stop 1. A V_b vein with garnet in Underhill schist is located on the top of the outcrop. (Sample location JR-73.)

7.3 STOP 3: Fairly large roadcut in Underhill schist on north side of Route 2. A V_e vein is found here, as are good examples of V_c veins with irregular forms. (Sample location JR-163.)

Turn around and proceed east on Route 2, back toward Waterbury.

8.2 Bolton - Waterbury line.

9.1 STOP 4: Park carefully along the right (south) side of Route 2 near the west end of a long, curving set of roadcuts on both sides of road. These are schists of the Hazens Notch formation just above the garnet isograd as mapped by Christman and Secor (1961). A large V_c vein is exposed on both sides of the road. (Location JR-4.)
Continue east on Route 2.

10.9 Junction of Routes 2 and 100N. Turn left (north) on to Route 100 toward Stowe.

11.0 (Middlesex quadrangle.)

12.0 (Stowe quadrangle.)

12.2 Turn right (east) on to Howard Avenue in Waterbury Center. Road is not well marked on Route 100 except for sign that points to Waterbury Center P. O. and Loomis Hill.

12.6 Turn left on to Maple Street after passing a crossroad at 12.5.

12.7 Turn right on to Loomis Hill Road.

13.1 Road bends to right, continue to stay on main road (paved).

14.6 Pavement ends, road continues as two-lane dirt road. Pass Ripley road to right and follow main road as is now travels north at the base of the Worcester Range.

16.0 Unmarked entrance to right (east) into an old amphibolite quarry.

16.1 STOP 5: Turn right into a parking lot marked with sign for the Waterbury trail to Mt. Hunger. Additional parking can be accessed by the unmarked entrance at mile 14.6. Follow old quarry road (and Mt. Hunger trail) northeast for about 100 feet, then veer off on one of several small unmarked paths that lead north about 50 feet to the top of the quarry. The walls of the quarry have many large loose blocks that look unstable and are best avoided. Exposed at the top is amphibolite of the Stowe formation and several generations of metamorphic veins. One mile to the east is pelitic schist with the assemblage sillimanite-kyanite-staurolite-garnet-biotite-muscovite-quartz. (Stop 5 is location JR-89, but data from JR-188 will be discussed.)
Return to parking area, turn right (north) back on to dirt road (which immediately narrows to one lane with only infrequent turnouts).

17.2 Barnes Hill Road comes in from left. Continue straight (north) on what has now become Stowe Hollow Road and widened back to two lanes. Follow this until it meets Gold Brook Road in Stowe Hollow.

19.0 Turn left (west) on to Gold Brook Road and follow it to Route 100.

20.2 Stop sign at Route 100. Turn right (north) on to Route 100 and follow it through Stowe.

23.7 Stagecoach Road forks off to left from Route 100. Snow's snack bar is just beyond fork. Make left turn on to Stagecoach Road and follow it north toward Morristown.

25.0 (Hyde Park 15" quadrangle.)

29.2 Stop sign - continue straight.

30.5 Stagecoach Road ends at stop sign, near Lake Lamoille. Turn left (north) toward Hyde Park.

31.7 One-lane bridge as you approach Hyde Park. Proceed with caution.

31.8 Stop sign. Turn left on to Main Street in Hyde Park and proceed to Route 15.

32.3 Stop sign. Turn left on to Route 15 and go northwest past Johnson.

38.3 Road to Ithiel Falls forks to right off of Route 15 just before a green iron bridge over the Lamoille River. Take this right fork on to unmarked road (only sign shows direction of Long Trail).

39.4 STOP 6: Turn left into parking area on left (southwest) side of road, across from roadcut. The road is narrow and visibility is poor, so be careful crossing road to outcrop. Good examples of V_b and V_c veins in biotite-grade Hazens Notch schist are found here. (Location JR-114.)
Reverse direction of travel, go back toward Route 15.

39.8 STOP 7: Pull off into parking area on right (southwest) side of road. Walk 0.15 mile southeast and downhill along road to outcrops of the Hazens Notch formation on left (northeast) side. Present here are excellent examples of F_b isoclinal folds of S_0, with superimposed F_c folds and V_c veins. (Location JR-113.)
Return to cars, continue back to Route 15.

40.5 Junction with Route 15. Go left (east) on Route 15, toward Johnson.
Continue east on Route 15 past Johnson and Hyde Park.

48.6 Junction of Routes 15 and 100S. Continue east on Route 15 toward Wolcott.

53.7 (Hardwick 15" quadrangle.)

55.3 To the right is a road to the town of Elmore - just before the road is a sign for "Hilltop X-country Ctr". Just beyond this road are roadcuts on both sides of Route 15.

55.35 STOP 8 (time allowing): Turn left into the parking area on the north side of Route 15, next to a large roadcut in the Moretown member of the Missisquoi formation. Seen here are some pull-apart structures within which have grown V_c veins. (Location JR-67.)

Reverse direction of travel on Route 15 and go short distance to road to Elmore.

55.4 Turn left (south) onto road to Elmore. Go across bridge over Lamoille River and follow the "main" travelled way (which is dirt most of the way and is a washboard on the steeper parts).

55.9 Road bends sharply to right.

56.8 (Hyde Park 15" quadrangle.)

57.4 Road bends sharply to left.

58.2 Stop sign at Route 12 in Elmore, Lake Elmore directly across road. Turn left (south) on to Route 12.

59.3 STOP 9: Turn sharply right on to small dirt road and park on either side (we will be continuing south on Route 12, so you will eventually have to turn around). Walk uphill (north) about 0.2 mile on Route 12 to a low outcrop of Stowe amphibolite partially hidden in overgrowth on right (east) side. Samples of V_c and V_e veins from here are discussed in the text. (Location JR-66.)

Go back to Route 12 and turn right to continue south toward Montpelier, passing through Worcester and Putnamville.

60.3 (Montpelier 15" quadrangle.)

71.0 Worcester.

73.5 Putnamville.

78.2 Coming into Montpelier. Route 12 is called Elm Street here. Continue straight on Elm Street until it runs into State Street.

79.4 Route 12 turns to left, but continue straight to avoid downtown traffic.

79.7 Turn right (west) on to State Street (Business Route 2), go past Capital Building to Bailey Ave. and follow signs to I-89.

80.1 Traffic light at Bailey Ave. Turn left on to Bailey and follow signs to I-89.

70.2 Traffic light at Memorial Drive. Turn right on to Memorial and work your way over into left lane so you can get onto I-89 South.

81.0 Get on I-89 South (toward White River Junction).

81.8 Roadcut with exposure of RMC on left side. (Barre 15" quadrangle.)

83.7 Take Exit 7 to right (Barre exit). Keep to right.

84.7 Traffic light at Berlin Corner. Turn right on to Paine Tpk.

84.95 Turn right at road junction to follow Paine Tpk.

85.3 Underpass below I-89.

85.35 Turn left on to dirt road (still marked as Paine Tpk.)

85.4 STOP 10: Park on right side of dirt road, next to large roadcuts on both sides. F_a and F_b folds in the Barton River member of the Waits River formation can be seen here, as well as S_a, V_a, and S_b. At the south end of the roadcut, basin-and-dome interference structures between F_b and F_{b+1} are developed on an exposed S_a surface. (Location JR-106.)

SUMMARY - end of trip

Return in the direction from which you came.

85.45 Turn right on paved road.

85.85 Turn left at stop sign.

86.1 Traffic light. You have a choice of going right to get to Barre or the Barre-Montpelier Road or going left to get back on to I-89.